Climate change and the growth of Amazonian species seedlings: an ecophysiological approach to *Euterpe oleracea*

Genilda Canuto Amaral, José Eduardo Macedo Pezzopane, Rogério de Souza Nóia Júnior, Mariana Duarte Silva Fonseca1, Manuel Fernández Martínez, Vanessa de Oliveira Gomes, João Vitor Toledo, José Ricardo Macedo Pezzopane, Raúl Tapias Martín

Abstract

Climate change threatens many native species of the Amazon rainforest. Among the endangered species is açaí (*Euterpe oleracea*), a species of great national and international interest due to the nutritional benefits and medicinal properties of its fruit. However, information on the ecophysiological responses of açaí to climate change is still lacking. Therefore, the objective of this study was to evaluate the effect of increased temperature and changes in CO2 concentration on the ecophysiology of açaí seedlings. To this end, açaí seedlings were subjected, for 90 days, to three different climate scenarios: current Amazonian conditions; RCP4.5 (current average temperature in the Amazon + 2.5 °C and 538 ppm carbon dioxide concentration, i.e., CO2); and RCP8.5 (+ 4.5 °C and 936 ppm CO2 concentration). In addition, two irrigation levels were applied in each climate scenario: seedlings were maintained at 90% (without stress) and 40% (with stress) of the substrate's water-holding capacity. Gas exchange, water status, fluorescence parameters, enzymatic antioxidant activity, and dry matter production were evaluated. High CO2 concentration improved açaí gas exchange (increasing its assimilation), regardless of water availability and substrate temperature. However, high temperature and high vapor pressure deficit reduced quantum yield and increased minimum fluorescence and enzymatic antioxidant activity. Therefore, açaí seedlings did not convert the additional assimilated carbon (due to the higher CO2 concentration) into biomass, showing lower total dry matter accumulation for climate scenarios RCP4.5 and RCP8.5. Our results indicated that the positive impacts of increased CO2 concentration on gas exchange might not offset the negative impacts of increased air temperature and vapor pressure (VPD) on açaí growth.

Keywords: Amazon, Açaí, High CO2, Gas exchange, Temperature, Water stress

Introduction

The impacts of climate change on the planet have been the subject of public policy and economic debates worldwide. The Intergovernmental Panel on Climate Change (IPCC) estimates that the temperature could rise by up to 5.7 °C under the RCP8.5 scenario by the end of the 21st century, compared to the baseline period of 1850–1900 (IPCC, 2021). This temperature change could alter precipitation patterns (Kimball et al., 2001; Reich et al., 2016) and atmospheric vapor pressure deficit (VPD), resulting in various ecophysiological changes (ranging from cellular structure to morphology) in diverse plant species (Alvarenga et al., 2014; Duursma et al., 2014; Marenco et al., 2014).

Increased CO2 concentration has positive effects on photosynthesis (Way et al. 2015; Amaral et al. 2021) by stimulating the Rubisco carboxylation rate and decreasing photorespiration (Bernacchi et al. 2001; Sage and Kubien 2007), thus improving photosynthetic efficiency (Leakey et al. 2009). However, elevated temperatures intensify respiration, reduce chlorophyll synthesis, and accelerate its degradation (Mathur et al. 2014). Furthermore, temperature also affects stomatal conductance and causes leaf abscission (Taiz and Zeiger 2013; Neves et al. 2019). VPD also increases with high temperatures, further limiting stomatal processes (Costa and Marenco 2007) and photosynthesis (Marenco et al. 2014). However, the physiological processes of plants are also regulated by the availability of water in the soil, and plants under water limitation reduce stomatal conductance to maintain water potential (Guo et al. 2010; Noia Junior et al. 2019), which affects carbon assimilation (Farooq et al. 2009).

With climate change, heat waves and droughts will become more frequent and severe in the Amazon rainforest, which has implications for native species, especially in the early seedling stage. For example, rubber tree seedlings lose the ability to assimilate carbon after seven days subjected to temperatures above 40 °C (Noia Junior et al., 2018), and jaborandi growth was affected by high temperatures, even when cultivated under conditions of high atmospheric CO2 concentration (Amaral et al., 2021; Amaral et al., 2022). This raises concerns about the future of *Euterpe oleracea* (açaí), a species native to the Amazon (Yamaguchi et al., 2015), which has great global interest (Oliveira et al., 2016), due to the nutritional and medicinal properties of its fruits (Cantu-Jungles et al., 2017; Oliveira et al., 2019). The growing consumption of açaí stimulated a shift in the extractive production system to commercial plantations, starting a

process of expansion of the species to large commercial areas (Rufino et al. 2011). It is noteworthy that the reports in the literature only assess the effect of single climatic elements on açaí (Suresh et al. 2010; Oliveira et al. 2016, 2019; Silvestre et al. 2017; Silva et al. 2017; Rosa et al. 2019). However, açaí plants responses to climate change remains unknown, bringing uncertainty to its commercial production expansion, which ultimately depends on seedling survival after plantation.

Therefore, the objective of the study was to evaluate the effect of climate change by simulating three climate scenarios: the current Amazon and Representative Concentration Pathways 4.5 (RCP4.5) and 8.5 (RCP8.5), on the ecophysiology of açaí seedlings. Our hypothesis was that: (i) The predicted increases in CO2 concentration, air temperature, vapor pressure deficit, and water stress will cause a disruption of the homeostasis of physiological processes.; (ii) Although the photosynthesis process is benefited by the higher CO2 concentration, associated with the increase in temperature, the vapor-pressure deficit (VPD) and water stress will promote oxidative damage and decrease the efficiency of photosystem II, resulting in a reduction in seedling growth. Thus, we consider that knowing the physiological responses of açaí conducted in different climatic scenarios will provide advantages such as: (i) Understanding on the future of the species under different climate change scenarios; (ii) Assisting in the conservation of the species; and (iii) improve physiological knowledge in the early stages of the species in a warm climate.

Material and methods

Experimental conditions

This study was conducted at the experimental area of the Federal University of Espírito Santo, Brazil (latitude 20°47′25″ S, longitude 41°23′48″ W, and altitude 120 m). The experiment was carried out in three greenhouses (Van der Hoeven®) with automated environmental control, from June 23 to September 23, 2018. Three different climate scenarios were simulated in the automated greenhouses, with controlled air temperature and humidity, and atmospheric carbon dioxide (CO_2) concentration. Each scenario was simulated in a different greenhouse. Within each climate scenario, two open-roof chambers (OTCs) were used.

The current scenario in the Amazon was constructed considering the minimum, mean, and maximum air temperatures (Tair), relative humidity (RH), and vapor pressure deficit (VPD) of the city of Manaus, Amazonas state. This region has (humid tropical rainforest climate (Af) according to the Köppen classification (Alvares et al. 2013). These data were obtained through the average of the historical climate data from 1980 to 2010 (30 years), from the National Meteorological Institute (INMET). Microclimate conditions in this scenario were maintained by the evaporative cooling system (pad cooling), air conditioners and heaters. VPD was obtained through the difference between the water vapor saturation pressure (*es*) and the partial water vapor pressure (*ea*). The *es* was calculated from the Tetens equation, and the ea by the product between the RH and *es*.

The other two scenarios simulate climate change and were based on the scenarios proposed by the UN Intergovernmental Panel on Climate Change (IPCC), built by its member institutions (Pinheiro et al. 2014), consisting of the fifth phase of the Coupled Model Intercomparison Project (CMIP5) (Taylor et al. 2012). A new set of scenarios called Representative Concentration Pathways (RCPs) was used in the IPCC's Fifth Assessment Report (AR5), which serve as input for climatic modeling and atmospheric chemistry in the numerical experiments of CMIP5. The RCPs comprise four emission scenarios which lead to four levels of radiative forcing in 2100, and the number of each scenario is given according to the forcing value in W/m2, namely 2.6, 4.5, 6.0 and 8.5 (IPCC 2021). Thus, the RCP4.5 scenario, considered intermediate, in which the forcing stabilizes, and the RCP8.5 scenario of high emission and a low technological level of mitigation were used, where the forcing continues to increase after 2100 (IPCC 2021).

The Tair and VPD variation curves for the RCP4.5 and RCP8.5 scenarios were simulated from the increased projected values of future climate scenarios based on the climate norm values for Manaus (Central Amazon). Climate change projections for the RCP4.5 and RCP8.5 scenarios show an increase in the mean annual Tair temperature of 2.5 and 4.5 °C, respectively, for the Manaus region (Supplementary Fig. S1). The CO2 concentration values for the scenarios in these projections were 538 ppm for RCP4.5 and 936 ppm for RCP8.5 (IPCC, 2013). The air temperature of the greenhouses was controlled by an evaporative cooling system (pad cooling), air conditioners and heaters which were activated by temperature controllers (Full GaugeR, MT-543Ri plus). Relative humidity values were maintained by using humidity

controllers (Full GaugeR, AHC-80 plus) which are based on psychrometry (difference between dry bulb and wet bulb) to measure the relative humidity of the air, in addition to a fogger nozzle fogging system. Considering that VPD only varies with temperature and relative humidity (both controlled), VPD values were also controlled in the greenhouses.

Variations in temperature and relative humidity values were controlled and maintained using SistradR software. The temperature was adjusted every 30 minutes during the day and every hour at night to simulate daily environmental conditions in each greenhouse in the study (Supplementary Fig. S1), while a fixed value was programmed for the desired humidity.

Pots containing açaí seedlings grown from seed (more details in the "Experimental Design and Measurements" subsection) were placed in open-roof chambers (ORCs) to expose them to different concentrations of atmospheric CO2. The ORCs are cylindrical, composed of two parts (upper and lower), and each OR has a forced air injection system with internal CO2 and CO2 flow regulators (Supplementary Fig. S2). The CO2 injection system was turned on daily at 8:00 a.m. and turned off at 5:00 p.m. In addition, the CO2 concentration inside each OTC was monitored at 8 am and 12 pm using a CO2 analyzer (Testo Sensor, model 535) during the experiment.

Automatic weather stations were installed inside the greenhouses to characterize the microclimate in each scenario (Table 1). The stations consisted of CS500 temperature and relative humidity sensors (Campbell Scientific Inc., Logan, UT, USA). Data were stored on a CR-10× data logger (Campbell Scientific, Inc., Logan, UT, USA), with readings taken every ten seconds and averaged every five minutes. Two levels of water availability were established to assess plant tolerance to water stress in each scenario, characterized as: well-watered seedlings (considered the control: unstressed) and water-stressed seedlings (40% of the substrate's maximum water-holding capacity: stressed). The two irrigation levels were based on studies by Silvestre et al. (2016, 2017).

The maximum water retention capacity of the substrate (MWRC) was subsequently calculated to characterize the two water availability levels as follows: a substrate sample was collected before adding to the pots (control sample). The control sample was saturated with water and after free heavy drainage to characterize the saturated weight. After weighting, the control sample was taken to a forced circulation oven at a temperature of 105 °C for 24 h to characterize its dry weight. Thus, the MWRC value was calculated using the equation below:

$$MWRC = Wps - Wp - [(Wsp \cdot Wds/Ws])$$

In which, Wps is the weight of the pots with saturated substrate (g); Wp is the weight of the empty pots (g); Wsp is the weight of the substrate inserted in the pots (g); Wds is the weight of the dry control sample (g); Ws is the weight of the saturated control sample (g).

The MWRC of all pots used in the experiment was determined using Eq. 1 using the Wvs of each pots. The irrigation control was performed by daily weighing of the experimental units and the water lost through evapotranspiration was replaced when necessary (Freire et al. 1980). The water content of the substrate was evaluated daily to measure the water retention capacity (WRC) tested as a treatment, irrigated seedlings (Not stressed) were maintained with substrate moisture at 90% of WRC, and seedlings subjected to water stress (Stressed) were maintained at 40% of the substrate WRC.

Experimental design and measurements

The experiment was conducted over a period of 90 days in a completely randomized design within each climate scenario (current Amazonia, RCP4.5 and RCP8.5) reproduced separately in different greenhouses and containing two levels of water availability within each greenhouse, thus totaling six treatments with six replicates each. Four-month-old *Euterpe oleracea* seedlings (average height ± SE, 19 ± 3.5 cm) were transplanted into white pots with a capacity of five liters and dimensions of 17 × 22 × 17 cm, filled with a commercial substrate (composed of bio-stabilized pine bark, vermiculite, charcoal grinder, water, and phenolic foam). Then, 4.8 g/L of a controlled fertilizer was added to the substrate, containing the following nutrients: macronutrients (15% nitrogen, 8% phosphorus, 12% potassium, 1.2% magnesium, 4% sulfur) and micronutrients (0.4% iron, 0.02% boron, 0.02% zinc, 0.05% copper, 0.06% manganese, and 0.015% molybdenum). This ensured that there were no nutrient deficiencies that could affect seedling growth. After transplanting, the seedlings were kept for 30 days in conditions similar to the natural environment of the species (current Amazon) and then were randomly distributed into the scenarios (current Amazon, RCP4.5 and RCP8.5). The variable responses of the physiological parameters and growth were then determined after 90 days of monitoring under the different treatments.

Determination of gas exchange and water status of the leaves

The net CO2 assimilation rate (*A*, μmol m^{-2} s^{-1}), transpiration rate (*E*, mmol H2O m^{-2} s^{-1} of H2O), stomatal conductance (*gs*, mol m^{-2} s^{-1} of H2O) and intracellular CO2 concentration (*Ci*, μmol mol^{-1}) were measured using a portable infrared gas analyzer (IRGA, model Li COR 6400, LI-COR Inc., Lincoln, NE, USA), with 6 cm2 measuring chamber. A fixed light intensity of 1500 μmol m^{-2} s^{-1} (provided by the light source of the LI-6400-02B) and a reference CO2 concentration of 400, 538 and 936 μL L^{-1} were used in the Current Amazon, RCP4.5 and RCP8.5 scenarios, respectively. Measurements were carried out at the following times: 8 am, 10 am, 12 pm and 3 pm on fully expanded leaves of the upper third of the plant, six seedlings were used for each treatment. Each seedling was considered a replicate. The instantaneous carboxylation efficiency (*A*/*Ci*, μmol m^{-2} s^{-1}/μmol mol^{-1}) was established through the relationship between the net CO2 assimilation rate and the intercellular CO2 concentration, and the intrinsic efficiency of water use (*A*/*gs*, μmol CO2 mol^{-1} H2O) was established through the relationship between the net CO2 assimilation and stomatal conductance rate.

Leaf water potential was measured at two times: at 4 am and at 12 pm using a Scholander 1505D-EXP model pressure chamber (PMS Instrument Co., Albany, OR, USA). Water potential was measured on fully expanded leaves from the upper third of all plants in each treatment.

Fluorescence and chlorophyll parameters

Quantum yield (Fv/Fm) and initial fluorescence (F0) were measured using a FluorPen model FP 100 (Photon Systems Instruments, Brno, Czech Republic). Measurements were performed on healthy, fully expanded leaves from the upper middle third of the plant, adapted to darkness for 30 minutes and to a saturating light pulse of 1500 μmol m^{-2} s^{-1}. Data were collected on three leaves of each seedling at two times: at 4 am (pre-dawn) and at 12 pm (highest incidence of solar radiation).

Chlorophyll was characterized using chlorophyll a and b indices, measured in fully expanded leaves from the upper third of the plant, using six plants per treatment and taking two readings for each plant. Each seedling was considered a replicate. Chlorophyll index readings were

taken using a chlorophyll meter (ChlorofiLOG R, model CFL 1030, Falker). ClorofiLOGR provides results in dimensionless units of FCI values (Falker Chlorophyll Index) (Falker 2008). Determination of enzymatic antioxidants activity Samples of fully expanded leaves were taken from the upper third of the plant (between 10:30 am and 11:30 am) to analyze enzymatic antioxidants activity. The crude enzymatic extracts were obtained following Peixoto et al. (1999).

Superoxide dismutase (SOD, EC 1.15.1.1) activity was determined following Del Longo et al. (1993), with the reaction mixture (2.97 mL) composed of 50 nM potassium phosphate buffer (pH 7.8), 13 mM methionine, 75 µM p-nitro tetrazolium blue, 0.1 mM ethylene diaminetetraacetic acid and 2 µM riboflavin. The reaction started with the addition of 30µL of crude enzyme extract. Subsequently, the reading was taken in the spectrophotometer with an absorbance of 560 nm, and activity was conferred to the formazan blue compound produced by the photo-reduction reaction of p-nitro tetrazolium blue (Giannopolitis and Ries 1977). Unitary SOD activity was defined as the enzyme content to inhibit 50% of the photoreduction reaction of the p-nitro tetrazolium blue (Beauchamp and Fridovich 1971).

The catalase (CAT, EC 1.11.1.6.) activity was determined following of Havir and Mchale (1987). The reaction mixture (2.9 mL) consisted of 50 mM potassium phosphate buffer (pH 7.0) and 12.5 mM hydrogen peroxide. The reaction was started by adding 100 µL of the enzyme extract. The extract reaction was evaluated in a Multiskan Go model UV−Visible spectrophotometer (Thermo Scientific, Multiskan GO, Finland) at 25 ^{o}C in absorbance at a wavelength of 240 nm at two times, being in the first seconds and in the first minute of the reaction. CAT activity was quantified based on the molar extinction coefficient of hydrogen peroxide (36 mM cm^{-1}), according to Anderson et al. (1995).

The evaluation of pyrogallol peroxidase (POX, EC 1.11.1.7) was determined based on the purpurogalin production at 420 nm at 25 ^{o}C (Kar and Mishra 1976). The reaction mixture (2.9 mL) was composed of 25 nM potassium phosphate buffer solution (pH 6.8), 20 mM pyrogallol and 20 mM hydrogen peroxide; the reaction started with the addition of 100 µL of the extract enzymatic. The reading was taken at the first minute of the reaction to determine the activity of POX, and was then calculated taking into account a molar extinction coefficient of purpurogalin 2.47 36 mM cm−1 (Chance and Maehly 1955).

Growth evaluation

The growth variables evaluated at the end of the experiment were: height, measured with a millimeter ruler; total leaf area (LA), measured with a LI-3100 leaf area integrator (Li-Cor Inc., Lincoln, Nebraska, USA); shoot dry mass (SDM); and root dry mass (RDM). Seedlings were sectioned into shoots (leaves and stems) and roots to measure dry mass production. The roots were washed to remove the substrate using a fine-mesh sieve to reduce losses. Subsequently, the shoots and roots were packed separately in paper bags and placed in a forced-air oven at 65 °C until a constant weight was reached (72 h). Total dry mass (TDM) was quantified by summing the SDM and RDM values.

The growth variables evaluated at the end of the experiment were: height, measured with the aid of a millimeter ruler; total leaf area (LA), measured using a LI-3100 leaf area integrator (Li-Cor Inc, Lincoln, Nebraska, USA), shoot dry mass (SDM) and root dry mass (RDM). The seedlings were sectioned into shoots (leaves and stems) and roots in order to measure dry mass production. The roots were washed to remove the substrate with a fine mesh sieve to reduce losses. Then, the shoots and roots were packed separately in paper bags and put in a forced air circulation oven at 65 °C until constant weight was obtained (72 h). The total dry mass (TDM) was quantified by the sum of the SDM and RDM values.

Statistical analysis

Statistical analyses were performed using R software (R Core Team 2017), ExpDes.pt package (Ferreira et al. 2014). All data were subjected to analysis of variance (ANOVA), and means were compared using Tukey's test ($p \leq 0.05$) to assess the interaction between climate scenarios and water availability levels. The normality and homogeneity of the data ($p \leq 0.05$) were analyzed using the Shapiro-Wilk test (1965) and Hartley's F-test (1950). Interaction graphs between the climate scenario (current Amazonia, RCP4.5, and RCP8.5) and water availability levels were plotted when significant. When the interaction was not significant, climate scenarios were compared by grouping the two irrigation treatments, and all ANOVA results are presented in Supplementary Tables S1–S5.

Results

Gas exchange and water status

Gas exchange in açaí seedlings was influenced by the interaction between climate scenarios and water availability ($p \leq 0.05$, Supplementary Table S1) (Fig. 1). Higher rates of net CO2 assimilation (A) were observed throughout the day in CO2-enriched scenarios in well-watered seedlings, especially in the RCP8.5 scenario. The highest A value was observed at 8:00 h, where well-watered seedlings and those exposed to the RCP8.5 scenario showed 38% and 46% more A than in the current Amazon scenario, respectively. Seedlings in the RCP8.5 scenario maintained higher A activity throughout the day, even under water stress. Water-stressed seedlings grown in the RCP4.5 scenario reduced A activity by 48% between 8:00 h and 10:00 h (Fig. 1 a, b).

Seedlings grown in the RCP4.5 and RCP8.5 scenarios showed lower stomatal conductance (*gs*) values throughout the day, regardless of water availability. The highest *gs* values were observed in the current Amazon scenario. Intracellular CO2 (Ci) and A concentrations were favored by the higher CO2 scenarios, RCP4.5 and RCP8.5. The results showed that Ci values were, on average, 54% higher in seedlings in the RCP8.5 scenario (Fig. 1e, f) compared to those in the current Amazon scenario.

Our results indicate that, during the warmest hours of the day, 12 p.m. and 3 p.m. (Fig. 1 g, h), transpiration rates in açaí seedlings were reduced in CO_2-enriched environments (RCP4.5 and RCP8.5), regardless of water availability levels. However, an increase in water use efficiency (E) was observed in well-watered seedlings in the Amazonian scenario. Furthermore, when comparing stressed and unstressed seedlings, water stress resulted in a 77% reduction in E at 10 a.m.

Intrinsic water use efficiency (*A*/*gs*) increased under RCP 4.5 and RCP 8.5 conditions (Fig. 1 i, j). Well-watered açaí seedlings in the RCP8.5 scenario exhibited a 70% higher *A*/*gs* at 8 a.m. than well-watered seedlings in the current Amazonian scenario. While water-stressed seedlings in the RCP8.5 scenario exhibited a 65% higher *A*/*gs* at 12 p.m. than water-stressed seedlings in the current Amazonian scenario. Instantaneous carboxylation efficiency (A/Ci) was lower in the RCP8.5 scenario than in the other scenarios studied, for both water level treatments (Fig. 1 k, l). In the current Amazonian scenario, water-stressed seedlings exhibited a higher A/Ci throughout the day.

The water potential of açaí seedlings under RCP4.5 and RCP8.5 scenarios was more negative at 4 am than the observed in the current Amazon scenario seedlings (Fig. 2A). Furthermore, the RCP8.5 scenario was the most stressful for the açaí seedlings (Fig. 2B) at 12 pm, with greater water potential compared to the other scenarios studied (Supplementary Table S2).

Fluorescence and chlorophyll parameters

No statistically significant differences were observed between water availability treatments in the different climate scenarios (Supplementary Table S3). At 4:00 a.m., no statistically significant differences were found in quantum yield (Fv/Fm) in the studied climate scenarios (Fig. 3A). On the other hand, the environmental conditions of the RCP8.5 scenario negatively affected the açaí seedlings at 12:00 p.m., showing a 17% reduction in Fv/Fm compared to the current Amazonian conditions (Fig. 3B).

Minimum fluorescence (F0) values were affected by the scenarios at both evaluation times. Seedlings under the RCP8.5 scenario showed the highest F0 values at both times (Fig. 3D). Likewise, the RCP4.5 scenario did not influence açaí fluorescence, as it showed no differences compared to the current Amazonian conditions. Finally, only F0 showed a significant difference in water availability levels at 12:00 p.m., where well-watered seedlings showed the lowest values.The chlorophyll of açaí seedlings was also affected by the studied scenarios ($p < 0.001$, Fig. 4, Supplementary Table S3). Chlorophyll *a* of the leaves of the seedlings was attenuated under the conditions of the RCP8.5 scenario (Fig. 4A), showing a 17% reduction in leaf pigments. Chlorophyll *b* decreased under RCP8.5 (Fig. 4B), unlike RCP4.5, in which chlorophyll *b* presented the highest value. In the RCP4.5 scenario, the chlorophyll *b* of the seedlings was 56% higher than the seedlings in the RCP8.5 scenario. In this scenario, the chlorophyll *b* of the seedlings was 56% higher than the seedlings under RCP8.5 scenario.

Enzymatic antioxidant activity

The production of superoxide dismutase (SOD) and catalase (CAT) enzymes was affected by the climatic scenarios and the water availability levels ($p \leq 0.02$, Fig. 5A and B, Supplementary Table S4). The lowest SOD enzymatic activity occurred in RCP8.5 for not stressed seedlings, with a reduction of 53% in relation to the RCP 4.5 scenario. The pyrogallol peroxidase enzyme

(POX) activity did not differ between climatic scenarios and showed an average activity of 1595 mmol min^{-1} g DM.

Water availability levels in each scenario affected the activity of the three enzymes studied. The effect of water stress was least pronounced on SOD activity in seedlings under scenario RCP4.5 (Fig. 5A), affecting 15% of the enzyme's antioxidant activity compared to well-watered seedlings. The scenario with the greatest effect of irrigation was RCP8.5, in which water-stressed seedlings showed a 68% increase in SOD production compared to well-watered seedlings.

Water availability levels affected CAT activity, most significantly in scenario RCP4.5 (Fig. 5B). Water-stressed seedlings in this scenario showed a 97% increase in CAT activity. On the other hand, the activity of this enzyme was less affected by water stress when seedlings were subjected to scenario RCP8.5. Water availability levels also affected POX activity, as water-stressed açaí seedlings showed 25% more activity than those under well-watered conditions.

Seedling growth

Seedlings grown under the RCP4.5 climate scenario showed the greatest growth in height and leaf area (Fig. 6A and B, Supplementary Table S5). In addition, açaí seedlings showed a reduction of 13% and 29% in height and leaf area under the RCP8.5 scenario, respectively. The highest total dry mass (TDM) production values were observed in the current Amazon and RCP4.5 scenarios in well-watered seedlings ($p \leq 0.03$, Fig. 7, Supplementary Table S5). For water-stressed seedlings, the TDM production under the conditions of the RCP4.5 and RCP8.5 scenarios was on average 11% higher than in the current Amazon (Fig. 7A). Note that the effect of water stress was more pronounced in the current Amazon climate scenario, in which water-stressed seedlings showed a 53% reduction in TDM production compared to well-watered seedlings.

On the other hand, açaí seedlings under water stress, presented in the RCP 8.5 scenario, showed a 28% reduction in shoot dry matter (SDM) production compared to well-irrigated seedlings. Shoot dry matter (SDM) production of well-irrigated seedlings was higher in the current Amazon and RCP4.5 scenarios ($p < 0.01$, Fig. 7B). Seedlings from the RCP8.5 climate scenario showed a 39% reduction in SDM production compared to the current Amazon

scenario, while water-stressed seedlings in the RCP 8.5 scenario showed a 21% reduction in SDM compared to well-irrigated seedlings.

The root dry mass (RDM) showed the same trend as the TDM and SDM variables ($p \leq 0.01$, Fig. 7C). The root system was negatively affected in water stress conditions in all of the studied scenarios. Water stress had a more pronounced effect in the current Amazon, in which the root growth of water-stressed seedlings reduced 58% in relation to well-watered seedlings.

Discussion

Our results revealed the effect of climate change scenarios with high CO2 concentration, air temperature, and VPD (potential deposition), associated with different levels of soil water availability, on gas exchange, fluorescence, enzymatic antioxidant activity, and the growth of açaí seedlings cultivated in the Amazon region. A beneficial effect on gas exchange was observed with increasing CO2 concentration in climate scenarios RCP4.5 and RCP8.5. However, total seedling dry biomass production was significantly reduced, intensified by water stress. These results indicate that the combined effect of increased CO2 concentration with high temperatures and VPD could decrease net primary production.

Gas exchange responses to climate change

Gas exchange in açaí seedlings revealed stimulation caused by increased atmospheric CO2 concentration in the RCP4.5 and RCP8.5 scenarios, under different water deficit treatments (Fig. 1). The net CO2 assimilation rate (A) and, consequently, the intracellular CO2 concentration (Ci) were higher in the RCP 4.5 and RCP 8.5 scenarios, compared to current Amazonian conditions. The higher A and Ci may be related to the activation of Rubisco due to the increased CO2 concentration, which is the main substrate of the Calvin cycle (Urban et al. 2019). This indicates that the beneficial effects of increased CO2 on gas exchange in açaí seedlings outweighed the stressful conditions caused by high temperature (Neves et al. 2019), high VPD (Jiao et al. 2019), and low water availability (Noia Junior et al. 2019). The beneficial effect of high CO2 concentration on açaí is consistent with the results found by several authors (Dikšaitytė et al. 2019; Urban et al. 2019; Jiao et al. 2019).

In addition to the increase in A, there was a decrease in stomatal conductance (*gs*), reducing transpiration (E), especially in seedlings under water stress. This was also due to the increase

in CO2 (Leakey et al. 2009), which resulted in an increase in intrinsic water use efficiency (*A*/*gs*). However, instantaneous carboxylation efficiency (A/Ci) decreased, indicating limitations in Rubisco activity (Niinemets et al. 2009). These results may indicate that water-stressed plants needed to invest more in non-structural carbohydrates than in structural carbon for biomass in order to cope with the water deficit, which can cause downregulation of photosynthesis in response to high CO2 levels (Jimenez et al. 2013; Tissue et al., 1993, 2001). In addition, the decreased Instantaneous carboxylation efficiency (*A*/*Ci*) in water-stressed plants, may indicate limitations to Rubisco activity (Niinemets et al. 2009). Similar results have also been reported by other authors for Açaí (Oliveira et al. 2019) and for other palm trees (Oliveira et al. 2016; Suresh et al. 2010; Silva et al.
2017).

Fluorescence and chlorophyll parameters as affected by climate change

Climatic conditions and water stress also affected fluorescence parameters. We observed that seedling stress increased with CO_2, temperature, and DPV, leading to an increase in quantum yield (Fv/Fm) and minimum fluorescence (F0), and affecting chlorophylls (a and b). Under optimal plant growth conditions, Fv/Fm values range from 0.77 to 0.81 (Murchie and Lawson, 2013; Zha et al., 2017). The Fv/Fm at 4:00 a.m. was greater than 0.8, indicating no damage to photosystem II (PSII) at that time. However, Fv/Fm decreased to around 0.5 at 12 pm under RCP 8.5 scenario, and considering that Fv/Fm is a measure of the electron transfer chain efficiency of the PSII (Wu et al. 2018), its low measured values, may indicate the inactivation of PSII photochemistry (Adams et al. 2013).

Our results also show an increase in F0 (Fig. 3), which may indicates that heat dissipation occurred in an uncontrolled manner caused by stomatal closure and increased water potential (Fig. 1 and 2), producing an excess of excitation within the leaves (Thwe and Kasemsap 2014). In addition, this increase in F0 could indicate structural changes in the antenna pigments such as dissociation of the pigments from the light-collecting antennas of the PSII main complex (Mishra and Terashima 2003; Mishra et al. 2007).

Chlorophylls *a* and *b* were significantly reduced in the RCP8.5 scenario, demonstrating that increased CO2, temperature, and VPD reduced photon absorption by the leaves. According to the literature, higher CO2 concentrations reduce chlorophyll content (Ceulemans and

Mousseau 1994; Wullschleger et al. 1992), increase the accumulation of inactive or damaged photosystem II reaction centers (Jordan et al. 2016; Šprtova et al. 2003; Kalina et al. 2001), and/or modify thylakoid membrane proteins involved in electron transport (Hideg and Strid 2017). Increased temperature reduces chlorophyll content (Hasanuzzaman et al. 2013; Mathur et al. 2014; Perdomo et al. 2017). Silvestre et al. (2017) reported that açaí seedlings grown under water stress conditions had a reduced chlorophyll content, as also indicated in this study.

Enzymatic antioxidants activity under climate change scenarios

The results of enzymatic antioxidants activity demonstrated that there was an increase in POX, SOD and CAT enzymes, mainly for water-stressed seedlings. These enzymes are part of the antioxidant defense system of plants, are related to their tolerance to abiotic stress, and play an important protective role against the harmful effects of ROS, such as O_2^-, H_2O_2, and OH_2^- (Mittler, 2002). Several studies demonstrate that plants protect themselves against the effects of ROS under adverse conditions thanks to increased activity of antioxidant enzymes (Li et al., 2017; He et al., 2014). Increased concentration of POX, SOD and CAT enzymes, as found here for Açaí seedlings under water stress conditions, indicates high ROS production, causing oxidative stress to the plants (Li et al. 2017). Similar results have also been reported by Tang et al. (2018) in evaluating *Cucumis sativus* L., Soni and Abdin (2017) in studying *Artemisia annua* L., Omidi et al. (2018) in *Lallemantia ibérica*, and Wang et al. (2019) in *Prunus persicae* L.

Climate change will affect açaí ecophysiology in Amazon forest

Climatic scenarios and water stress affected the growth of Açaí seedlings. Our results indicated a beneficial effect on gas exchange caused by the increased CO2, however total dry mass decreased, particularly under RCP 8.5. This indicated that growth is not only determined by carbon assimilation capacity, but also by the interaction of many other factors, such as respiration rate, assimilate translocation efficiency, and leaf area (Marenco and Lopes, 2005). Our results indicated that açaí growth and production in the Amazon region could be threatened by future climate change, even with increased gas exchange rates due to rising CO2 levels.

As hypothesized, increased CO2 concentration, air temperature, VPD and water stress associated with climate change disrupt the homeostasis of physiological processes in açaí

seedlings. Despite the benefits of increased CO2 concentration for açaí photosynthesis, warmer temperatures, along with high VPD and water stress, promote oxidative damage and decrease the efficiency of photosystem II, affecting seedling growth..

Conclusion

Our results highlight the impact of climate change on the growth of açaí seedlings in the Amazon region. We reveal that the positive impacts of increased CO2 concentration on gas exchange may not offset the negative impacts of increased air temperature and water vapor pressure (VPD) on açaí growth under conditions without water deficit. However, increased CO2 concentration minimized the impacts of water deficit stress on açaí growth. These results provide an important foundation for future studies aimed at protecting native species in the Amazon region from the threat of climate change. Future studies focusing on forest regeneration and restoration, plantation survival and yield, and the development of açaí clones with greater ecophysiological capacity to grow in complex environments could benefit from the findings of this study.

Acknowledgements This work is supported by *FAPES* (Research Support Foundation of Espirito Santo) with research funding and doctoral scholarships to the first author (Edital PROCAP 2016).

References

Adams WW, Muller O, Cohu CM, Demming-Adams B (2013) May photoinhibition be a consequence, rather than a cause, of limited plant productivity? Photosynth Res 117(1–3):31–44. https:// doi. org/ 10.1007/ s11120- 013- 9849-7

Alvarenga CB et al (2014) Effect of the water vapor pressure deficit in the air on hydropneumatic spraying of artificial targets. Biosci J 30(1):182–193

Alvares CA, Stape JL, Sentelhas PC, Goncalves JLM, Sparovek G (2013) Koppen's climate classification map for Brazil. Meteorol Z. https:// doi. org/ 10. 1127/ 0941- 2948/ 2013/ 0507

Amaral GC, Pezzopane JEM, Noia Junior RS, Fonseca MDS, Toledo JV, Xavier TMT, Oliveira BS, Martinez MF, Jeronimo Junior RAC, Goncalvez EO (2021) Ecophysiology of *Pilocarpus microphyllus* in response to temperature, water availability and vapour pressure deficit. Trees 35(543–555):2020. https:// doi. org/ 10. 1007/ s00468- 020- 02055- xTrees

Amaral GC et al (2022) *Pilocarpus microphyllus* seedling growth threatened by climate change: an ecophysiological approach. Theor Appl Climatol 147:347–361. https:// doi. org/ 10. 1007/ s00704- 021- 03831-6

493 Anderson MD, Prasad TK, Stewart CR (1995) Changes in Isozyme profiles of catalase, peroxidase, and
494 glutathione reductase during acclimation to chilling in mesocotyls of maize seedlings. Plant Physiol
495 109(4):1247–1257. https:// doi. org/ 10. 1104/ pp. 109.4. 1247
496 Beauchamp C, Fridovich I (1971) Superoxide dismutase: improved assay applicable to acrylamide gels.
497 Anal Biochem 44:276–287
498 Bernacchi CJ, Singsaas EL, Pimentel C, Portis AR Jr, Long SP (2001) Improved temperature response
499 functions for models of Rubisco-limited photosynthesis. Plant Cell Environ 24:253–259. https:// doi.
500 org/ 10.1111/j. 1365- 3040. 2001. 00668.x
501 Cantu-Jungles TM, Iacomini M, Cipriani TR, Cordeiro LMC (2017) Extraction and characterization of
502 pectins from primary cell walls of edible Açaí (*Euterpe oleraceae*) berries, fruits of a monocotyledon
503 palm. Carbohyd Polym 158:37–43. https:// doi. org/ 10. 1016/j. carbp ol. 2016. 11. 090
504 Ceulemans BR, Mousseau M (1994) Effects of elevated atmospheric CO2 on woody plants. New
505 Phytologist Trust 127(3):425–446
506 Chance B, Maehly AC (1955) Assay of catalases and peroxidases: methods in enzymology. Academic
507 Press 2:764–775
508 Costa GF, Marenco RA (2007) Fotossintese, condutancia estomatica e potencial hidrico foliar em arvores
509 jovens de andiroba (Carapa guianensis). Acta Amaz 37(2):229–234 de Oliveira HO, de Castro GL,
510 Correa LO, Silvestre WV, do Nascimento SV, da Silva Valadares RB, Oliveira GC, Santos RI, Festucci-
511 Buselli RA, Pinheiro HA (2019) Coupling physiological analysis with proteomic profile to
512 understand the photosynthetic responses of young *Euterpe oleracea* palms to drought. Photosynth
513 Res 140:189–205. https:// doi. org/ 10. 1007/ s11120- 018- 0597-6
514 Del Longo OT, Gonzalez CA, Pastori GM, Trippi VS (1993) Antioxidant defences under hyperoxygenic
515 and hyperosmotic conditions in leaves of two lines of maize with differential sensitivity to drought.
516 Plant Cell Physiol 34(7):1023–1028
517 Dikšaitytė A, Viršilė A, Žaltauskaitė J, Januškaitienė I, Juozapaitienė G (2019) Growth and
518 photosynthetic responses in Brassica napus differ during stress and recovery periods when exposed
519 to combined heat, drought and elevated CO2. Plant Physiol Biochem 142:59–72. https:// doi. org/ 10.
520 1016/j. plaphy. 2019.06. 026
521 Duursma RA, Barton CVM, Lin Y-S, Medlyn BE, Eamus D, Tissue DT, Ellsworth DS, McMurtrie RE
522 (2014) The peaked response of transpiration rate to vapour pressure deficit in field conditions can be
523 explained by the temperature optimum of photosynthesis. Agric for Meteorol 189–190:2–10.
524 https://doi. org/ 10. 1016/j. agrfo rmet. 2013. 12. 007
525 Falker (2008) Automacao agricola. Manual do medidor eletronico de teor clorofila (ClorofiLOG/CFL
526 1030). Porto Alegre, p. 33
527 Farooq M, Wahid A, Kobayashi N, Fujita D, Basra SMA (2009) Plant drought stress: effects mechanisms
528 and management. Sustain. Agric. Springer Netherlands, Dordrecht, pp 153–188. https:// doi. org/
529 10.1007/ 978- 90- 481- 2666-8_ 12
530 Ferreira EB, Cavalcanti PP, Nogueira DA (2014) ExpDes: An R Package for ANOVA and experimental
531 designs. Appl Math 5(19):2952–2958. https:// doi. org/ 10. 4236/ am. 2014. 519280
532 Freire JC, Ribeiro MAV, Bahia VG, Lopes AS, Aquino LH (1980) Respostas do milho cultivado em casa
533 de vegetacao a niveis de agua em solos da regiao de Lavras (MG). Rev Bras Cienc Solo 4:5–8

534 Giannopolitis CN, Ries SK (1977) Superoxide dismutases: I., occurrence in higher plants. Plant Physiol
535 59:309–314
536 Guo X-Y, Zhang X-S, Huang Z-Y (2010) Drought tolerance in three hybrid poplar clones submitted to
537 different watering regimes. J Plant Ecol 3(2):79–87. https:// doi. org/ 10. 1093/ jpe/ rtq007
538 Hartley HO (1950) The use of range in analysis of variance. Biometrika 37(3/4):271. https:// doi. org/
539 10.2307/ 23323 80
540 Hasanuzzaman M, Nahar K, Alam M, Roychowdhury R, Fujita M (2013) Physiological, biochemical,
541 and molecular mechanisms of heat stress tolerance in plants. Int J Mol Sci 14(5):9643–9684. https://
542 doi.org/ 10. 3390/ ijms1 40596 43
543 Havir EA, Mchale NA (1987) Biochemical and developmental characterization of multiple forms of
544 catalase in tobacco leaves. Plant Physiol 84:450–455
545 He Y, Yang J, Zhu B, Zhu Z (2014) Low root zone temperature exacerbates the ion imbalance and
546 photosynthesis inhibition and induces antioxidant responses in tomato plants under salinity. J Integr
547 Agric 13(1):89–99. https:// doi. org/ 10. 1016/ s2095- 3119(13) 60586-9
548 Hideg E, Strid A (2017) The effects of UV-B on the biochemistry and metabolism of plants. In: Jordan
549 BR (ed) UV-B radiation and plant life: molecular biology to ecology. CABI, Wallingford, pp 90–110
550 IPCC (2013) Summary for policymakers. In: Climate change 2013: The physical science basis.
551 Contribution of Working Group I to the Fifth Assessment Report of the Intergovernmental Panel on
552 Climate Change.In: TF Stocker, D Qin, G-K Plattner, M Tignor, SK Allen, J Boschung, A Nauels, Y
553 Xia, V Bex, PM Midgley, (Eds.). Cambridge University Press Cambridge, United Kingdom, New
554 York, NY, USA 1–30
555 IPCC (2021) Climate Change 2021: The physical science basis. Contribution of Working Group I to the
556 Sixth assessment report of the intergovernmental panel on climate change. In: Masson-Delmotte,
557 V.,P. Zhai, A. Pirani, S.L. Connors, C. Pean, S. Berger, N. Caud, Y. Chen, L. Goldfarb, M.I. Gomis, M.
558 Huang, K. Leitzell, E. Lonnoy, J.B.R. Matthews, T.K. Maycock, T. Waterfield, O. Yelekci, R. Yu, and
559 B. Zhou (eds.). Cambridge University Press. In Press
560 Jiao X-C, Song X-M, Zhang D-L, Du Q-J, Li J-M (2019) Coordination between vapor pressure deficit and
561 CO2 on the regulation of photosynthesis and productivity in greenhouse tomato production. Sci Rep
562 9(1):8700. https:// doi. org/ 10. 1038/ s41598- 019- 45232-w
563 Jimenez S, Dridi J, Gutierrez D, Moret D, Irigoyen JJ, Moreno MA, Gogorcena Y (2013) Physiological,
564 biochemical and molecular responses in four Prunus rootstocks submitted to drought stress. Tree
565 Physiology 33:1061–1075. https:// doi. org/ 10. 1093/ treep hys/ tpt074
566 Jordan B, Strid A, Wargent J (2016). What role does UVB Play in determining photosynthesis?
567 Handbook of Photosynthesis, 3rd edition, Edition: 3rd edition, Chapter: Chapter 16: 275–286.
568 Doi:https:// doi. org/10. 1201/ b19498- 21
569 Kalina J, Urban O, Čajanek M, Kurasova I, Špunda V, Marek MV (2001) Different responses of Norway
570 spruce needles from shaded and exposed crown layers to the prolonged exposure to elevated CO2
571 studied by various chlorophyll a fluorescence techniques. Photosynthetica 39(3):369–376
572 Kar M, Mishra D (1976) Catalase, peroxidase, and polyphenoloxidase activities during rice leaf
573 senescence. Plant Physiol 57:315–319

574 Kimball BA et al (2001) Elevated CO2, drought and soil nitrogen effects on wheat grain quality. New
575 Phytol 150(2):295–303
576 Leakey ADB, Ainsworth EA, Bernacchi CJ, Rogers A, Long SP, Ort DR (2009) Elevated CO2 effects on
577 plant carbon, nitrogen, and water relations: six important lessons from FACE. J Experim Botany
578 60(10):2859–2876. https:// doi. org/ 10. 1093/ jxb/ erp096
579 Li J, Cang Z, Jiao F, Bai X, Zhang D, Zhai R (2017) Influence of drought stress on photosynthetic
580 characteristics and protective enzymes of potato at seedling stage. J Saudi Soc Agric Sci 16(1):82–88.
581 https:// doi. org/ 10. 1016/j. jssas. 2015. 03. 001
582 Marenco RA, Antezana-Vera SA, Gouvea PR, Camargo MA, Oliveira MF, Santos JK (2014) Fisiologia de
583 especies florestais da Amazonia: fotossintese, respiracao e relacoes hidricas. Rev Ceres 61:786–799.
584 https:// doi. org/ 10. 1590/ 0034- 737x2 01461 000004
585 Marenco RA, Lopes NF (2005). Fisiologia Vegetal: Fotossintese, respiracao, relacoes hidricas e
586 nutricaomineral. 451p
587 Mathur S, Agrawal D, Jajoo A (2014) Photosynthesis: Response to high temperature stress. J
588 PhotochemPhotobiol B: Biol 137:116–126
589 Mishra AN, Terashim, I (2003). Changes in photosystem activities during adapta-tion of Vicia faba
590 seedlings to low, moderate and high temperature. Plant Cell Physiology, Annual Symposium
591 JSPP,pp 27–29
592 Mishra AN, Srivastava A, Strasser RJ (2007). Elastic and plastic responses of Viciafaba leaves to high
593 temperature and high light stress. In: Gordon conference on temperature stress in plants.
594 Ventura,USA, pp 25–30
595 Mittler R (2002) Oxidative stress, antioxidants and stress tolerance. Trends Plant Sci 7(9):405–410
596 Murchie EH, Lawson T (2013) Chlorophyll fluorescence analysis: a guide to good practice and
597 understanding some new applications. J Experim Botany 64(13):3983–3998. https:// doi. org/ 10. 1093/
598 jxb/ert208
599 Neves LH, Santos RIN, Teixeira GIS, Araujo DG, Silvestre WVD, Pinheiro HA (2019) Leaf gas exchange,
600 photochemical responses and oxidative damages in assai (Euterpe oleracea Mart) seedlings
601 subjected to high temperature stress. Sci Horticult 257:108733. https:// doi. org/ 10. 1016/j. scienta.
602 2019. 108733
603 Niinemets U, Diaz-Espejo A, Flexas J, Galmes J, Warren CR (2009) Importance of mesophyll diffusion
604 conductance in estimation of plant photosynthesis in the field. J Exp Bot 60(8):2271–2282. https://doi.
605 org/ 10. 1093/ jxb/ erp063
606 Noia Junior RS, Pezzopane JEM, Vinco JS, Xavier TMT, Cecilio RA, Pezzopane JRM (2018)
607 Characterization of photosynthesis and transpiration in two rubber tree clones exposed to thermal
608 stress. Brazilian J Bot 41(4):785–794. https:// doi. org/ 10. 1007/ s40415- 018- 0495-3
609 Noia Junior RS, Amaral GC, Pezzopane JEM, Fonseca MDS, Silva APC, Xavier TMT (2019)
610 Ecophysiological acclimatization to cyclic water stress in Eucalyptus. J Forestry Res 31(3):797–806.
611 https://doi. org/ 10. 1007/ s11676- 019- 00926-9
612 Oliveira LC, Oliveira MSP, Davide LC, Torres GA (2016) Karyotype and genome size in Euterpe Mart
613 (Arecaceae) species. Comparative Cytogenetics 10(1):17–25. https:// doi. org/ 10. 3897/ CompC
614 ytogen. v10i1. 5522

615 Omidi H, Shams H, Sahandi MS, Rajabian T, Miransari M (2018) Balangu (*Lallemantia* sp.) growth and
616 physiology under field drought conditions affecting plant medicinal content. Plant Physiol Biochem
617 130:641–646. https:// doi. org/ 10. 1016/j. plaphy. 2018. 08. 014
618 Peixoto PH, Cambraia J, Sant' Anna R, Mosquim PR, Moreira MA (1999) Aluminum effects on lipid
619 peroxidation and on the activities of enzymes of oxidative metabolism in sorghum. Rev Bras Fisiol
620 Veg 11(3):137–143
621 Perdomo JA, Capo-Bauca S, Carmo-Silva S, Galmes J (2017) Rubisco and Rubisco activase play an
622 important role in the biochemical limitations of photosynthesis in rice, wheat, and maize under high
623 temperature and water deficit. Front Plant Sci 8(13):490. https:// doi. org/ 10. 3389/ fpls. 2017. 00490/
624 full
625 Pinheiro JU, Neves JA, Cheves RE, Mendes D, Barreto NJC (2014). Avaliacao de Modelos do CMIP5 que
626 Melhor Expressam a Atuacao dos Vortices Ciclonicos em Altos Niveis (Vcans) no Nordeste Brasileiro
627 (NEB). Revista Brasileira de Geografia Fisica, 7(5), (Numero Especial-VIWMCRHPE):891–904
628 Reich PB, Sendall KM, Stefanski A, Wei X, Rich RL, Montgomery RA (2016) Boreal and temperate trees
629 show strong acclimation of respiration to warming. Nature 531:633–636. https:// doi. org/ 10. 1038/
630 natur e17142
631 Rosa BL, Souza JP, Pereira EG (2019) Increased atmospheric CO2 changes the photosynthetic responses
632 of Acrocomia aculeata (Arecaceae) to drought. Acta Botanica Brasilica 33(3):486–497. https:// doi.
633 org/ 10.1590/ 0102- 33062 019ab b0056
634 Rufino MSM, Perez-Jimenez J, Arranz S, Alves RE, de Brito ES, Oliveira MSP, Saura-Calixto F (2011)
635 Açaí (*Euterpe oleraceae*) 'BRS Para': a tropical fruit source of antioxidant dietary fiber and high
636 antioxidant capacity oil. Food Res Int 44(7):2100–2106. https:// doi. org/ 10. 1016/j. foodr es. 2010. 09.
637 011
638 Sage RF, Kubien DS (2007) The temperature response of C3 and C4 photosynthesis. Plant, Cell Environ
639 30(9):1086–1106
640 Shapiro SS, Wilk MB (1965) An analysis of variance test for normality (complete samples). Biometrika
641 52(3–4):591–611
642 Silva PA, Cosme VS, Rodrigues KCB, Detmann KSC, Leao FM, Cunha RL, Buselli RAF, Damatta FM,
643 Pinheiro HA (2017) Drought tolerance in two oil palm hybrids as related to adjustments in carbon
644 metabolism and vegetative growth. Acta Physiol Plant 39(2):58. https:// doi. org/ 10. 1007/ s11738-
645 017- 2354-4
646 Silvestre WVD, Pinehiro HA, Souza RORM, Palheta LF (2016) Morphological and physiological
647 responses of Açaí seedlings subjected to different watering regimes. Revista Brasileira De
648 Engenharia Agricola e Ambiental 20(4):364–371. https:// doi. org/ 10. 1590/ 1807- 1929/ agria mbi.
649 v20n4 p364- 371
650 Silvestre WVD, Silva PA, Palheta LF, de Oliveira Neto CF, Souza RORM, Festucci-Buselli RA, Pinheiro
651 HA (2017) Differential tolerance to water deficit in two Açaí (Euterpe oleracea Mart.) plant materials.
652 Acta Physiol Plant 39(1):4. https:// doi. org/ 10. 1007/ s11738- 016- 2301-9
653 Soni P, Abdin MZ (2017) Water deficit-induced oxidative stress affects artemisinin content and
654 expression of proline metabolic genes in Artemisia annua L. FEBS Open Bio 7(3):367–381. https://
655 doi. org/ 10. 1002/2211- 5463. 12184

Šprtova M, Špunda V, Kalina J, Marek MV (2003) Photosynthetic UV-B Response of Beech (Fagus sylvatica L) Saplings. Photosynthetica 41(4):533–543. https:// doi. org/ 10. 1023/b: phot. 00000 27517. 80915. 1b

Suresh K, Nagamani C, Ramachandrudu K, Mathur RK (2010) Gas-exchange characteristics, leaf water potential and chlorophyll a fluorescence in oil palm (Elaeis guineensis Jacq.) seedlings under water stress and recovery. Photosynthetica 48(3):430–436. https:// doi. org/ 10. 1007/ s11099- 010- 0056-x

Taiz L, Zeiger E, (2013) Fisiologia vegetal. 5. ed. Porto Alegre: Artmed, 918 p

Tang Y-Y, Yuan Y-H, Shu S, Guo S-R (2018) Regulatory mechanism of NaCl stress on photosynthesis and antioxidant capacity mediated by transglutaminase in cucumber (Cucumis sativus L.) seedlings. Scientia Horticulturae 235:294–306

Taylor KE, Stouffer RJ, Meehl GA (2012) An overview of CMIP5 and the experiment design. Bull Am Meteorol Soc 93:485–498

Thwe AA, Kasemsap P (2014) Quantification of OJIP fluorescence transient in tomato plants Under acute ozone stress. Nat Sci 48:665–675

Tissue DT, Thomas RB, Strain BR (1993) Long-term effects of elevated CO2 and nutrients on photosynthesis and rubisco in loblolly pine seedlings. Plant Cell Environ 16(7):859–65. https:// doi. org/ 10. 1111/j. 1365-3040. 1993. tb005 08

Tissue DT, Griffin KL, Turnbull MH, Whitehead D (2001) Canopy position and needle age affect photosynthetic response in field-grown *Pinus radiata* after five years of exposure to elevated carbon dioxide partial pressure. Tree Physiol 21(12–13):915–923. https:// doi. org/ 10. 1093/ treep hys/ 21. 12-13. 915

Urban O, Hrstka M, Holub P, Vesela B, Večeřova K, Novotna K, Grace J, Klem K (2019) Interactive effects of ultraviolet radiation and elevated CO2 concentration on photosynthetic characteristics of European beech saplings during the vegetation season. Plant Physiol Biochem 134:20–30. https:// doi. org/ 10. 1016/j. plaphy.2018. 08. 026

Wang X, Gao Y, Wang Q, Chen M, Ye X, Li D, Chen X, Li L, Gao D (2019) 24-Epibrassinolide-alleviated drought stress damage influences antioxidant enzymes and autophagy changes in peach (*Prunus persicae* L.) leaves. Plant Physiol Biochem 135:30–40. https:// doi. org/ 10. 1016/j. plaphy. 2018. 11. 026

Way DA, Oren R, Kroner Y (2015) The space-time continuum: the effects of elevated CO2 and temperature on trees and the importance of scaling. Plant Cell Environ 38:991–1007. https:// doi. org/ 10. 1111/ pce. 12527

Wu YJ, Ren C, Tian Y, Zha TS, Liu P, Bai YJ, Ma JY, Lai ZR, Bourquea CP-A (2018) Photosynthetic gasexchange and PSII photochemical acclimation to drought in a native and non-native xerophytic species (*Artemisia ordosica* and *Salix psammophila*). Ecol Ind 94:130–138

Wullschleger SD, Norby RJ, Hendrix DL (1992) Carbon exchange rates, chlorophyll content, and carbohydrate status of two forest tree species exposed to carbon dioxide enrichment. Tree Physiol 10(1):21–31. https://doi. org/ 10. 1093/ treep hys/ 10.1. 21

Yamaguchi KKL, Pereira LFR, Lamarao CV, Lima ES (2015) Amazon Açaí: chemistry and biological activities: a review. Food Chem 179:137–151

Zha T-S, Wu YJ, Jia X, Zhang MY, Bai YJ, Liu P, Ma JY, Bourque CP-A, Peltola H (2017) Diurnal response of effective quantum yield of PSII photochemistry to irradiance as an indicator of photosynthetic

acclimation to stressed environments revealed in a xerophytic species. Ecol Ind 74:191–197. https://
doi. org/ 10. 1016/j.ecoli nd. 2016. 11. 027

Table 1. Microclimatic characterization of the simulated scenarios in the air-conditioned greenhouses from June 23, 2018 to September 23, 2018. In which: T is the air temperature, RH is relative humidity and VPD is vapor-pressure deficit (minimum, mean and maximum)

Climatic variables	Current Amazon	RCP4.5	RCP8.5
	Air temperature (ºC)		
Tmin	23.9 (± 0.15)	24.5 (± 0.13)	26.7 (± 0.15)
Tmean	28.3 (± 0.14)	29.4 (± 0.13)	31.7 (± 0.15)
Tmax	32.9 (± 0.13)	34.3 (± 0.13)	36.7 (± 0.15)
	Relative Humidity (%)		
RHmin	81 (± 0.47)	47 (± 0.48)	29 (± 0.55)
RHmean	93 (± 0.39)	55 (± 0.47)	38 (± 0.56)
RHmax	98 (± 0.33)	62 (± 0.49)	46 (± 0.57)
	Vapor-Pressure Deficit (kPa)		
VPDmin	0.1 (± 0.01)	1.2 (± 0.02)	1.9 (± 0.04)
VPDmean	0.3 (± 0.01)	1.9 (± 0.02)	3.0 (± 0.04)
VPDmax	0.9 (± 0.01)	2.8 (± 0.02)	4.3 (± 0.04)

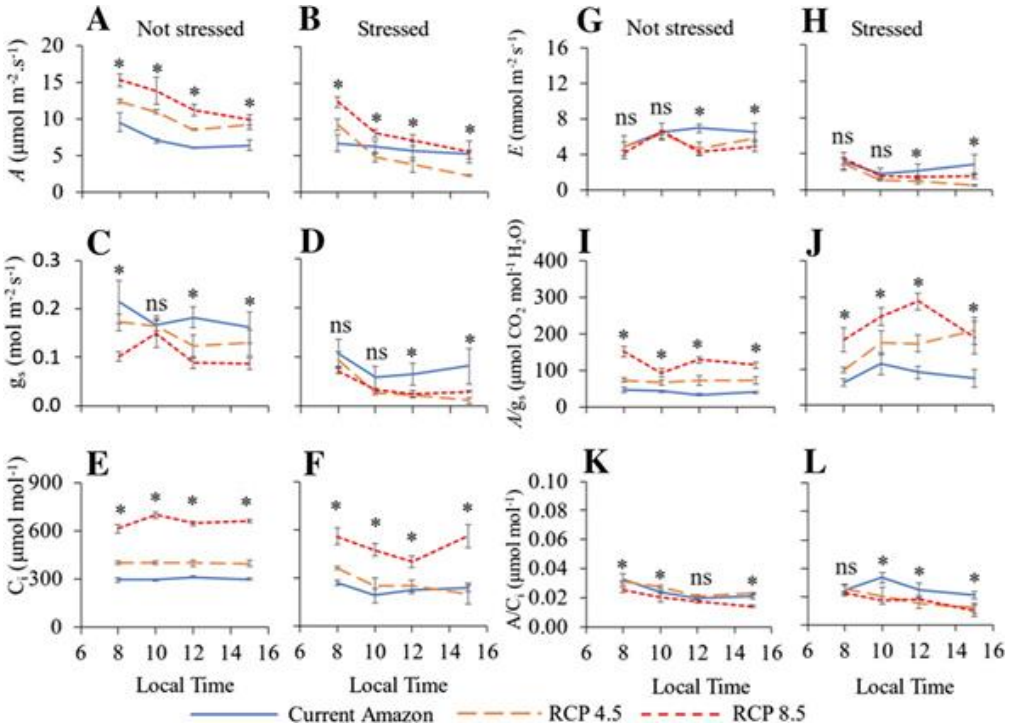

Figure 1. Net CO2 assimilation rate (*A*, a, b), stomatal conductance (*gs*, c, d), intracellular CO2 concentration (*Ci*, e, f), transpiration rate (*E*, g, h), intrinsic efficiency of water use (*A*/*Gs*, i, j) and instantaneous carboxylation efficiency (*A*/*Ci*, k, l) of açaí seedlings subjected to in different climatic scenarios (current Amazon, RCP4.5 and RCP8.5) and water availability levels: well-watered (Not stressed) and water-stressed (Stressed). Data are means ± standard deviation. ns: not significant, *: significant according to ANOVA, F < 0.05. The results from the analysis of variance (ANOVA) taking into account the effects of the different scenarios and water availability levels are presented in Supplementary Table S1.

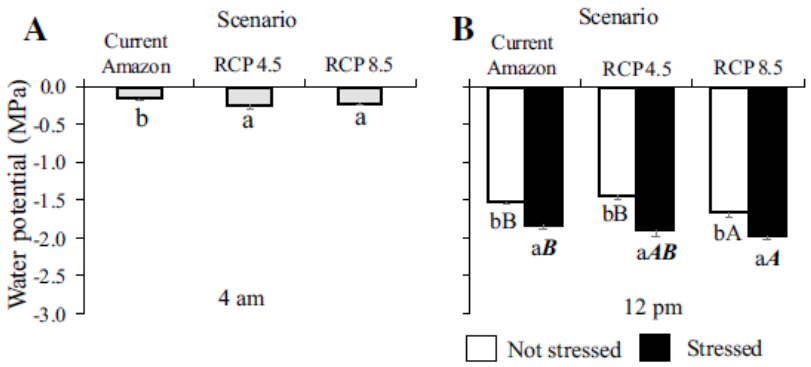

Figure 2. Water potential (A, 4 am and B, 12 pm) of Açaí seedlings subjected to different climatic scenarios (current Amazon, RCP4.5 and RCP8.5) and water availability levels: well-watered (Not stressed) and water-stressed (Stressed). Different letters represent statistically significant differences between treatments (Tukey, $p \leq 0.05$). For water potential at 12 pm (**B**), uppercase letters compare the statistical difference by climatic scenarios (upper case for not stressed and upper case bold/italic for stressed), and lowercase letters represent the statistical difference between water availability levels. Values represent means ± standard deviation. Graphs of the interaction between climate scenarios (current Amazon, RCP4.5, and RCP8.5) and water availability were plotted when the interaction was significant (panels with black and white bars); when the interaction was not significant, the climate scenarios (current Amazon, RCP4.5, and RCP8.5) were compared by combining both irrigation treatments (panels with gray bars). The results of the analysis of variance (ANOVA), considering the effects of the different scenarios and water availability levels, are presented in Supplementary Table S2.

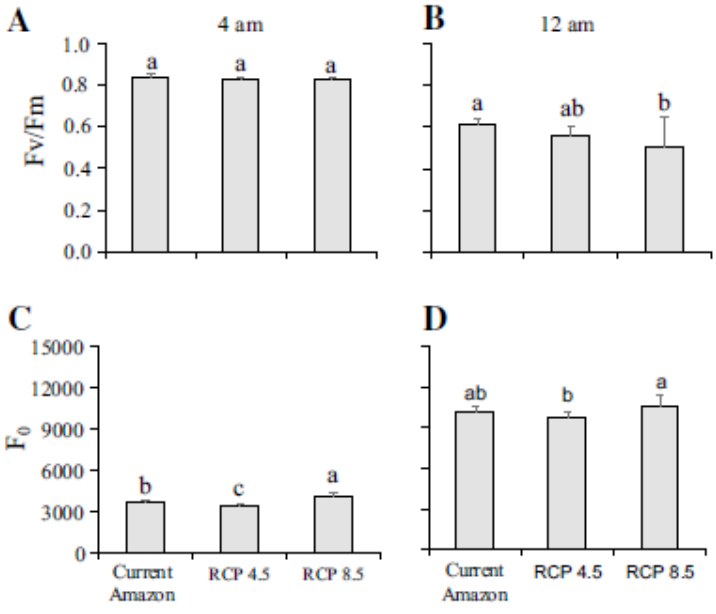

Figure 3. Quantum yield (Fv/Fm) and minimum fluorescence (F0) at 4:00 a.m. (A and C) and 12:00 p.m. (B and D) of açaí seedlings subjected to different climate scenarios (current Amazon, RCP4.5 and RCP8.5) and water availability levels: well-irrigated (no stress) and under water stress. Different letters represent statistically significant differences between treatments (Tukey, $p \leq 0.05$). Data are expressed as mean ± standard deviation. The results of the analysis of variance (ANOVA), considering the effects of the different scenarios and water availability levels, are presented in Supplementary Table S3.

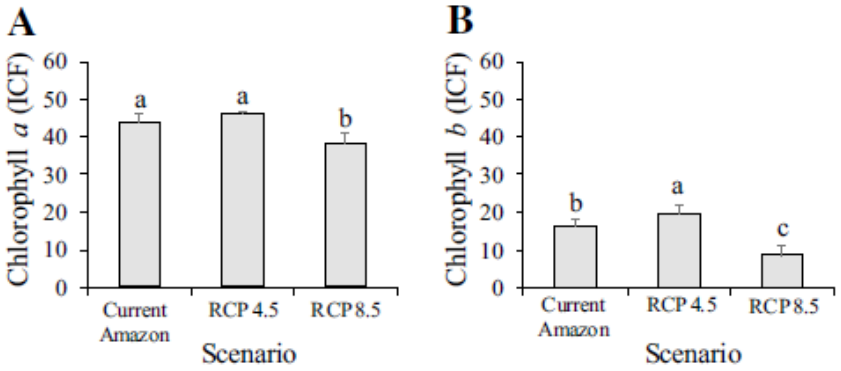

Figure 4. Chlorophyll *a* (**A**) and chlorophyll *b* (**B**) of açaí seedlings subjected to different climatic scenarios (current Amazon, RCP4.5 and RCP8.5) and water availability levels: well-watered (Not stressed) and water-stressed (Stressed). Different letters represent statistically significant differences between treatments (Tukey, $p \leq 0.05$). Data are means ± standard deviation. Values represent means ± standard deviation. The results from the analysis of variance (ANOVA) taking into account the effects of the different scenarios and water availability levels are presented in the Supplementary Table S3.

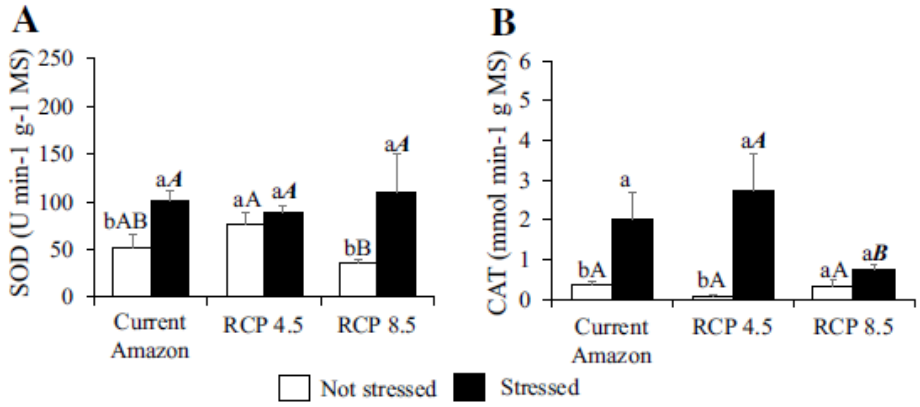

Figure 5. Effects of the antioxidant superoxide dismutase (A, SOD) and Catalase (B, CAT) enzymatic antioxidants activity of açaí seedlings subjected to different climatic scenarios (current Amazon, RCP4.5 and RCP8.5) and water availability levels: well-watered (Not stressed) and water-stressed (Stressed). Different letters represent statistically significant differences between treatments (Tukey, $p \leq 0.05$). Statistical differences between climate scenarios are represented by capital letters (uppercase for unstressed and bold/italic uppercase for stressed), and differences between water availability levels within each climate scenario are represented by lowercase letters. Values represent the mean ± standard deviation. The results of the analysis of variance (ANOVA), which considers the effects of the different scenarios and water availability levels, are presented in Supplementary Table S4.

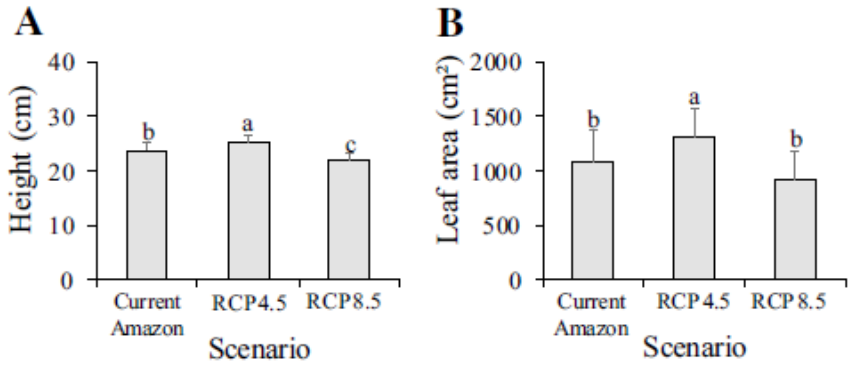

Figure 6. Height (**A**) and leaf area (**B**) of Açaí seedlings subjected to different climatic scenarios (current Amazon, RCP4.5 and RCP8.5) and water availability levels: well-watered (Not stressed) and water-stressed (Stressed). Different letters represent statistically significant differences between treatments (Tukey, $p \leq 0.05$). Data are means ⊚} standard deviation. Data are means ⊚} standard deviation. Values represent means ± standard deviation. The results from the analysis of variance (ANOVA) taking into account the effects of the different scenarios and water availability levels are presented in Supplementary Table S5.

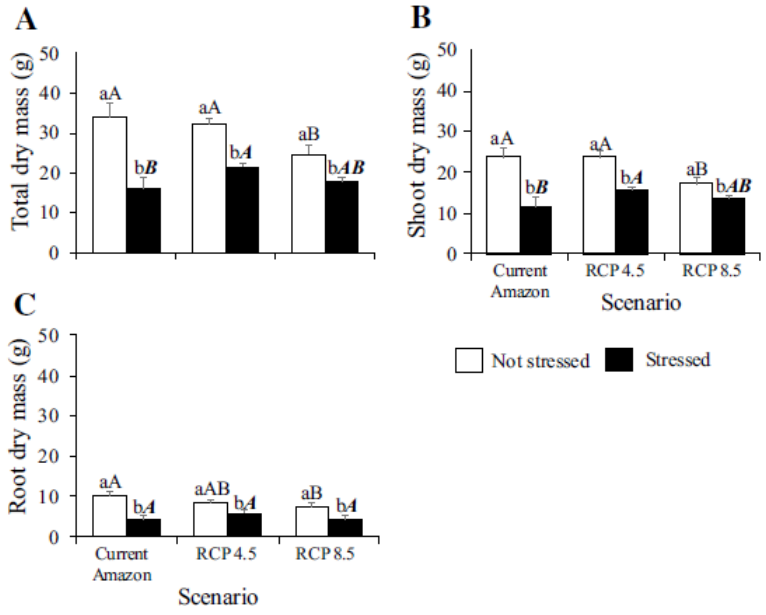

Figure 7. Total dry mass (**A**), shoot dry mass (**B**) and root dry mass (**C**) of Açaí seedlings subjected to different climatic scenarios (current Amazon, RCP4.5 and RCP8.5) and water availability levels: well-watered (Not stressed) and water-stressed (Stressed). Different letters represent statistically significant differences between treatments (Tukey, $p \leq 0.05$). Statistical differences between climate scenarios are represented by capital letters (uppercase for unstressed and bold/italic uppercase for stressed), and differences between water availability levels within each climate scenario are represented by lowercase letters. Values represent the mean ± standard deviation. The results of the analysis of variance (ANOVA), which considers the effects of the different scenarios and water availability levels, are presented in Supplementary Table S5.

Supplementary material

Figures

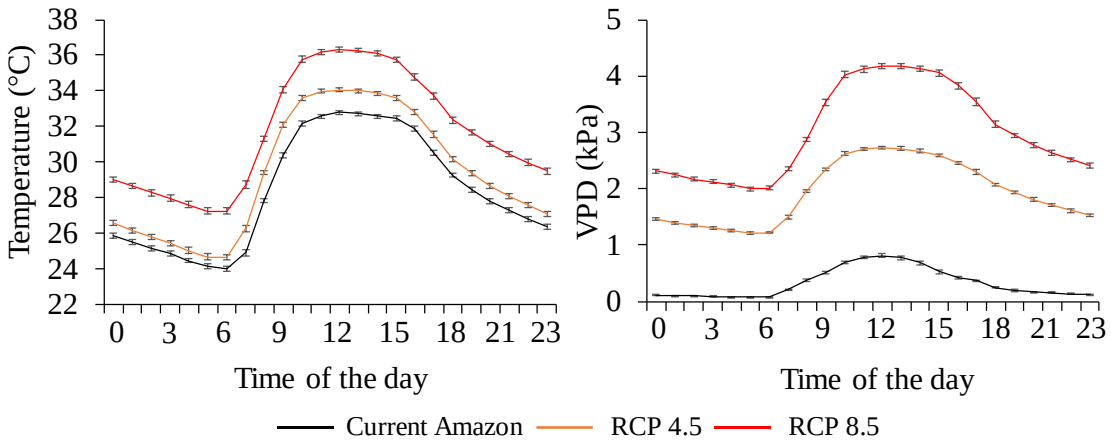

Figure S1. Hourly variations of air temperature and vapor-pressure deficit (VPD) of the three scenarios studied in greenhouses throughout the experimental period (June 23rd, 2018 to September 23rd, 2018). The data are mean ± standard error. Jerônimo Monteiro - ES, Brazil

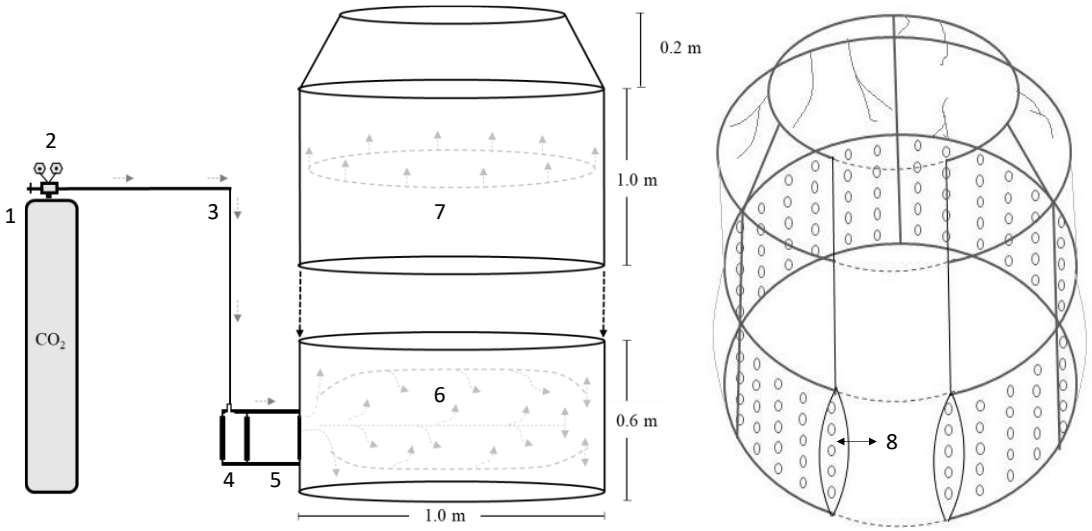

1: CO_2 cylinder; 2: CO_2 regulator; 3: pneumatic hose; 4: ventilation exhaust; 5: homogenization chamber; 6: lower part of the chamber; 7: upper part of the chamber; 8: coating detailing (double).

Figure S2. Schematic representation of the structure of open top chambers (OTCs) used to control atmospheric CO_2 concentration. Source: The author

Tables

Table S1. Net CO_2 assimilation rate (*A*), stomatal conductance (*gs*), intracellular CO_2 concentration (*Ci*), transpiration rate (*E*), intrinsic efficiency of water use (*A/Gs*) and instantaneous carboxylation efficiency (*A/Ci*) of açaí seedlings subjected to in different climatic scenarios (current Amazon, RCP4.5 and RCP8.5) and water availability levels: well-watered (Not stressed) and water-stressed (Stressed). Different letters represent statistically significant differences between treatments (Tukey, $p \leq 0.05$). The values are the mean values of each variable for the individual treatments.

Causes of variation	*A*	g_s	C_i	*E*	A/g_s	*A/Ci*
	μmol m^{-2} s^{-1}	mol m^{-2} s^{-1}	μmol mol^{-1}	mmol m^{-2} s^{-1}	μmol mol^{-1}	μmol m^{-2} s^{-1}
			8 am			
Scenario	54.38*	14.47*	198.46*	0.04 ns	69.86*	5.95*
Irrigation	43.17*	39.18*	8.66*	12.95*	9.58*	16.80*
Scenario x irrigation	0.023ns	3.60*	0.336 ns	0.91ns	0.22ns	1.02ns
			Scenario			
Current Amazon	8.10 c	0.16 b	282.00 c	3.97 a	54.74 c	0.03 a
RCP4.5	10.83 b	0.13 a	380.80 b	3.89 a	84.82 b	0.03 a
RCP8.5	13.85 a	0.09 a	586.81 a	3.83 a	166.16 a	0.02 b
			Water avalability levels			
Not stressed	12.41 a	0.16 b	435.29 a	4.60 a	89.58 b	0.03 a
Stressed	9.45 b	0.09 a	397.78 b	3.19 b	114.23 a	0.02 b
C.V. (%)	10.08	21.94	7.50	22.07	19.14	11.67
			10 am			
Scenario	36.31*	2.28 ns	162.08*	1.09 ns	26.58*	12.94*
Irrigation	98.11*	200.01*	96.14*	413.43*	117.55*	0.01 ns
Scenario x irrigation	16.05*	1.11 ns	4.52*	0.41ns	5.22*	9.50*
			Scenario			
Current Amazon	6.57 b	0.11 a	243.15 c	4.11 a	78.47 c	0.03 a
RCP4.5	7.86 b	0.09 a	323.97 b	3.69 a	120.36 b	0.02 b
RCP8.5	10.91 a	0.09 a	585.97 a	4.03 a	169.72 a	0.01 c
			Water avalability levels			
Not stressed	10.57 a	0.16 a	464.37 a	6.43 a	67.40 b	0.02 a
Stressed	6.33 b	0.04 b	304.35 b	1.46 b	178.30 a	0.02 a
C.V. (%)	12.40	20.80	10.36	15.17	20.39	16.41
			12 pm			
Scenario	31.32*	28.06*	177.30*	26.59*	123.33*	3.61 ns
Irrigation	65.17*	151.48*	189.94*	278.14*	196.59*	0.01 ns
Scenario x irrigation	12.59*	4.35*	16.11*	5.70*	15.33*	5.80*
			Scenario			
Current Amazon	5.80 b	0.12 a	268.80 c	4.54 a	62.12 c	0.02 a
RCP4.5	6.13 b	0.07 b	325.32 b	2.76 b	121.41 b	0.01 a
RCP8.5	9.18 a	0.05 b	523.37 a	2.85 b	207.78 a	0.01 a
			Water avalability levels			
Not stressed	8.59 a	0.13 a	452.38 a	5.26 a	77.17 b	0.01 a
Stressed	5.48 b	0.03 b	292.61 b	1.51 b	183.70 a	0.01 a

C.V. (%)	13.37	22.20	7.62	16.27	14.27	17.62
			15 pm			
Scenario	11.09*	12.36*	139.00*	8.58*	23.17*	19.92*
Irrigation	115.10*	60.95*	41.29*	138.39*	43.65*	17.02*
Scenario x irrigation	18.54*	2.69 ns	5.31*	2.92ns	5.59*	7.08*
			Scenario			
Current Amazon	5.75 b	0.12 a	270.09 b	4.66 a	57.04 b	0.02 a
RCP4.5	5.73 b	0.07 b	297.08 b	3.13 b	139.72 a	0.02 a
RCP8.5	7.68 a	0.05 b	612.21 a	3.16 b	150.51 a	0.01 b
			Water avalability levels			
Not stressed	8.41 a	0.12 a	452.93 a	5.68 a	75.23 b	0.02 a
Stressed	4.30 b	0.04 b	333.32 b	1.62 b	156.28 a	0.01 b
C.V. (%)	14.88	32.15	11.60	23.11	25.95	16.71

* = significant at the 5% probability level; ns = not significant; C.V. = coefficient of variation.

Table S2. Water potential at 4 am and 12 pm, respectively of açaí seedlings subjected to in different climatic scenarios (current Amazon, RCP4.5 and RCP8.5) and water availability levels: well-watered (Not stressed) and water-stressed (Stressed). Different letters represent statistically significant differences between treatments (Tukey, $p \leq 0.05$). The values are the mean values of each variable for the individual treatments.

Causes of variation	Water potential (MPa)	
	4 am	12 pm
Scenario	8.17*	13.07*
Irrigation	3.47 ns	178.52*
Scenario x irrigation	2.81 ns	3.66*
	Scenario	
Current Amazon	0.15 b	1.67 b
RCP4.5	0.24 a	1.67 b
RCP8.5	0.22 a	1.83 a
	Water avalability levels	
Not stressed	0.19 a	1.54 b
Stressed	0.22 a	1.90 a
CV%	20.90	3.86

* = significant at the 5% probability level; ns = not significant; C.V. = coefficient of variation.

Table S3. Quantum yield (Fv/Fm) and minimum fluorescence (F_0) at 4 am and 12 pm, respectively, and Chlorophyll *A* and *B* of açaí seedlings subjected to in different climatic scenarios (current Amazon, RCP4.5 and RCP8.5) and water availability levels: well-watered (Not stressed) and water-stressed (Stressed). Different letters represent statistically significant differences between treatments (Tukey, $p \leq 0.05$). The values are the mean values of each variable for the individual treatments.

Causes of variation	F_v/F_m		F_0		Chlorophyll (ICF)	
	4 am	12 pm	4 am	12 pm	*A*	*B*
Scenario	0.94 ^{ns}	3.86*	32.52*	4.42*	27.45*	47.67*
Irrigation	10.94*	5.24*	0.001 ^{ns}	7.47*	3.39^{ns}	3.92 ^{ns}
Scenario x irrigation	0.40 ^{ns}	3.11^{ns}	2.31^{ns}	0.11^{ns}	0.48^{ns}	0.45 ^{ns}
	Scenario					
Current Amazon	0.84 a	0.60 a	3623.00 c	10175.50 ab	43.83 a	16.25 b
RCP4.5	0.83 a	0.55 ab	3332.25 b	9757.00 b	46.06 a	19.64 a
RCP8.5	0.83 a	0.50 b	4061.12 a	10605.25 a	38.33 b	8.60 c
	Water avalability levels					
Not stressed	0.83 b	0.52 b	3673.00 a	9861.16 b	43.55 a	15.77 a
Stressed	0.84 a	0.59 a	3671.25 a	10497.33 a	41.94 a	13.89 a
CV%	0.66	12.96	4.96	5.60	5.03	15.62

* = significant at the 5% probability level; ns = not significant; C.V. = coefficient of variation.

Table S4. The activity of enzymatic antioxidants superoxide dismutase (SOD) and catalase (CAT), of açaí seedlings subjected to in different climatic scenarios (current Amazon, RCP4.5 and RCP8.5) and water availability levels: well-watered (Not stressed) and water-stressed (Stressed). Different letters represent statistically significant differences between treatments (Tukey, $p \leq 0.05$). The values are the mean values of each variable for the individual treatments.

Causes of variation	SOD	CAT
	U min^{-1} g^{-1} MS	mmol min^{-1} g MS
Scenario	0.49 ^{ns}	4.76*
Irrigation	32.83*	42.67*
Scenario x irrigation	4.98*	7.18*
	Scenario	
Current Amazon	76.69 a	1.20 ab
RCP4.5	82.75 a	1.41 a
RCP8.5	73.10 a	0.54 b
	Water avalability levels	
Not stressed	54.58 b	0.27 b
Stressed	100.45 a	1.84 a
CV%	25.30	55.76

* = significant at the 5% probability level; ns = not significant; C.V. = coefficient of variation.

Table S5. Growth variables of açaí seedlings subjected to in different climatic scenarios (current Amazon, RCP4.5 and RCP8.5) and water availability levels: well-watered (Not stressed) and water-stressed (Stressed). Different letters represent statistically significant differences between treatments (Tukey, $p \leq 0.05$). The values are the mean values of each variable for the individual treatments.

Causes of variation	Total dry mass	Shoot dry mass	Root dry mass	Height	Leaf area
	- - - - - - - - - - - - g - - - - - - - - - -			cm	cm^2
Scenario	8.29*	9.52*	4.95*	35.48*	13.82*
Irrigation	107.37*	95.11*	91.78*	54.21*	58.56*
Scenario x irrigation	8.28*	9.31*	5.68*	0.15 ns	0.29 ns
	Scenario				
Current Amazon	25.01 a	17.68 ab	7.32 a	23.87 b	1082.92 b
RCP4.5	26.86 a	19.74 a	7.12 ab	25.25 a	1321.70 a
RCP8.5	21.25 b	15.39 b	5.85 b	21.93 c	934.52 b
	Water avalability levels				
Not stressed	30.32 a	21.57 a	8.75 a	24.87 a	1345.16 a
Stressed	18.43 b	13.64 b	4.78 b	22.50 b	880.93 b
CV%	11.53	11.31	14.98	3.34	13.35

* = significant at the 5% probability level; ns = not significant; C.V. = coefficient of variation.